



1 Anomalous Amide Proton Chemical Shifts as Signatures of Hydrogen 2 Bonding to Aromatic Sidechains

3 Kumaran Baskaran^{*1}, Colin W. Wilburn^{*1}, Jonathan R. Wedell¹, Leonardus M. I. Koharudin², Eldon L.
4 Ulrich¹, Adam D. Schuyler¹, Hamid R. Eghbalnia¹, Angela M. Gronenborn², and Jeffrey C. Hoch¹

5 ¹Department of Molecular Biology and Biophysics, UConn Health, 263 Farmington Ave., Farmington, CT 06030-3305 USA

6 ²Department of Structural Biology University of Pittsburgh School of Medicine 3501 Fifth Ave., BST3/Rm. 1050 Pittsburgh, PA
7 15260 USA

8 Correspondence to: Jeffrey C. Hoch (hoch@uchc.edu)

9 Dedicated to Professor Robert Kaptein on the occasion of his 80th birthday.

10 **Abstract.** Hydrogen bonding between an amide group and the p- π cloud of an aromatic ring was first identified in a protein in the
11 1980s. Subsequent surveys of high-resolution X-ray crystal structures found multiple instances, but their preponderance was
12 determined to be infrequent. Hydrogen atoms participating in a hydrogen bond to the p- π cloud of an aromatic ring are expected
13 to experience an upfield chemical shift arising from a shielding ring current shift. We survey the Biological Magnetic Resonance
14 Data Bank for amide hydrogens exhibiting unusual shifts as well as corroborating nuclear Overhauser effects between the amide
15 protons and ring protons. We find evidence that Trp residues are more likely to be involved in p- π hydrogen bonds than other
16 aromatic amino acids, whereas His residues are more likely to be involved in hydrogen bonds with a ring nitrogen acting as the
17 hydrogen acceptor. The p- π hydrogen bonds may be more abundant than previously believed. The inclusion in NMR structure
18 refinement protocols of shift effects in amide protons from aromatic side chains, or explicit hydrogen bond restraints between
19 amides and aromatic rings, could improve the local accuracy of side-chain orientations in solution NMR protein structures, but
20 their impact on global accuracy is likely to be limited.

21 1 Introduction

22 In 1986, Perutz et al. (Levitt and Perutz, 1988) identified a putative hydrogen bond between an amino group of Asparagine and an
23 aromatic ring of a drug bound to hemoglobin. Similar observations of the π electrons of aromatic rings acting as acceptors for
24 hydrogen bonding have been reported before and since. (Klemperer et al., 1954; Mcphail and Sim, 1965; Knee et al., 1987) Later
25 in 1986, Burley and Petsko (Burley and Petsko, 1986) surveyed 33 high resolution protein structures and found further evidence
26 of aromatic hydrogen bonds. Tüchsen and Woodward (Tüchsen and Woodward, 1987) subsequently observed an upfield shift in
27 the Gly-37 NH and Asn-44 HN resonances due to a nearby Tyr-35 aromatic group. The measurements from this study allowed
28 Levitt and Perutz (Perutz, 1993) to estimate that these interactions contribute around 3 kcal mol⁻¹ in stabilizing enthalpy, about
29 half as strong as a conventional hydrogen bond. Further evidence of such H-bonding came from the 2001 study by Brinkley and
30 Gupta (Brinkley and B., 2001) showing FTIR spectroscopic evidence for hydrogen bonding between alcohols and aromatic rings.
31 The ability of aromatic rings to engage in weakly polar CH- π interactions is well documented, with NMR data from Plevin et
32 al. (Plevin et al., 2010) in the form of weak scalar (J) couplings between methyl groups and atoms in aromatic rings providing direct
33 evidence of these interactions. The study also included a survey of 183 X-ray structures and found 183 putative Me/ π interactions.
34 Brandl et al. (Brandl et al., 2001) surveyed 1154 protein structures from the Protein Data Bank (PDB (Consortium, 2019) for C-H
35 π H bonds and found 14,087 involving aromatic rings and satisfying their geometric criteria. This is made all the more impressive



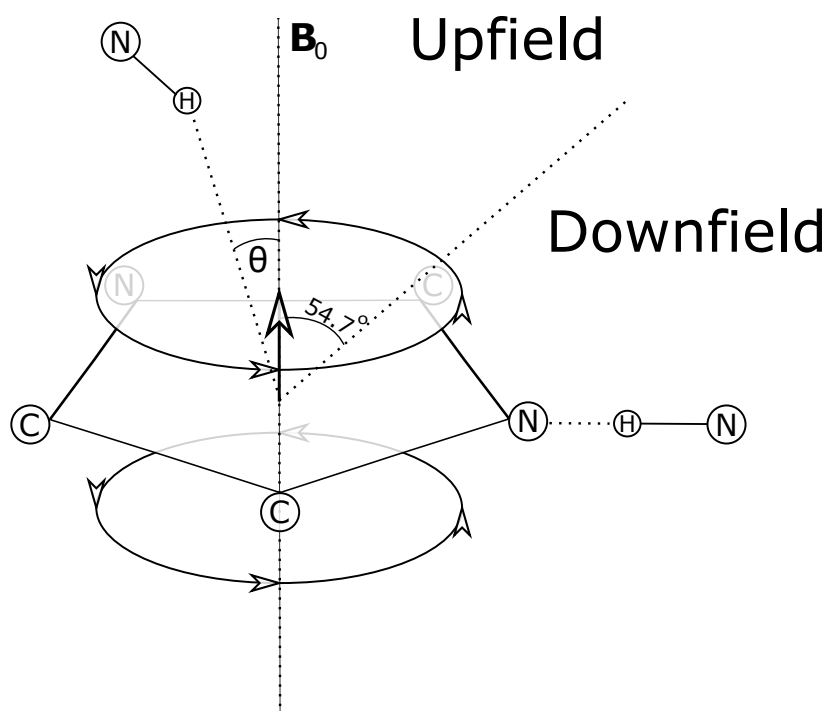
36 when considering that Levitt and Perutz report the partial charges on the C–H group are one third those on the N–H group (the
37 subject of this paper), suggesting that the interaction studied by Brandl et al. is correspondingly weaker. Another survey of note
38 was performed by Weiss et al. in 2010.(Weiss et al., 2001) This complete hydrogen bond analysis of two high resolution protein
39 structures from PDB found 50 C–H π and two (N,O)–H π bonds.

40 In addition to their ubiquity, there is some indication of the importance of these interactions. In a 1993 review, Perutz (Perutz,
41 1993) indicated the potentially wide-ranging importance of these interactions, particularly Armstrong et al.'s demonstration of
42 their role in stabilizing α -helices(Armstrong et al., 1993). There is also evidence that similar interactions play an important role in
43 protein-ligand complexes.(Panigrahi and Desiraju, 2007; Polverini et al., 2008)

44 Following the example of Tüchsen and Woodward (Tüchsen and Woodward, 1987) we seek to use NMR to provide corroborative
45 evidence of aromatic hydrogen bonds. In this paper, we survey the Biological Magnetic Resonance Bank (BMRB) for unusual
46 amide proton chemical shifts and amide-aromatic nuclear Overhauser effects.

47

48 Theoretical models for the geometrical dependence of the ring current shift include parameterization of quantum-mechanical(Haigh
49 and Mallion, 1979; Memory, 1963) calculations, semi-classical approximation using the Biot-Savart Law(Jackson, 1999) for the
50 field arising from current loops (Waugh and Fessenden, 1957; Jr. and Bovey, 1958), and a dipole approximation. For distances
51 from the ring center that are greater than 3 Å above the plane of the ring, and 5 Å in the plane of the ring, the theories all agree
52 well with a dipole approximation.(Hoch, 1983) The $(1-3\cos^2(\theta))/r^3$ geometrical dependence of the field arising from a magnetic
53 dipole (where θ is the angle between the vector from a proton to the aromatic ring center and the vector normal to the plane of the
54 ring) provides vivid explanation for cone separating upfield-shifted from down-field-shifted regions defined by $\theta=54.7^\circ$ (Figure
55 1).



56



57 **Figure 1.** Definition of the azimuthal angle (θ) and demarcation of regions of upfield and downfield ring current shifts.
58 For protons above the plane of a Tyr or Phe ring the upfield shift can reach 1.5 ppm for distances from the ring center around 3
59 Å; for protons in the plane of the ring the downfield shift approaches 2 ppm at 3 Å. For Trp the effects can be significantly larger.
60 Local mobility (e.g. fluctuations about the χ_2 side-chain dihedral angle of the aromatic residue) can substantially diminish ring
61 current shifts.²¹

62

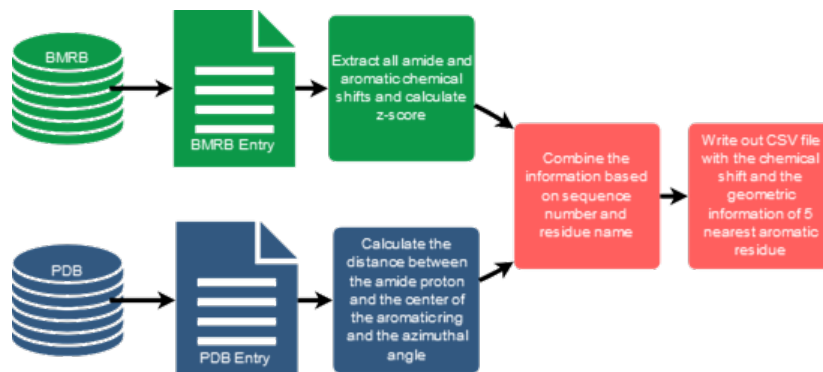
63 2 Approach

64 To investigate the connection between amide proton chemical shifts and the potential for hydrogen bonding to an aromatic ring,
65 we searched BMRB for assigned amide protons in proteins corresponding to structures deposited in the PDB. BMRB provides the
66 list of BMRB and PDB entry id pairs via BMRB API (http://api.bmrb.io/v2/mappings/bmrb/pdb?match_type=exact). As of Jan
67 2021 we found 7750 BMRB/PDB paired entries and retrieved the BMRB entries (in NMR-STAR format (Ulrich et al., 2019)) and
68 PDB entries (in mmCIF format (Bourne et al., 1997)) from their respective databases. We filtered out DNA/RNA entries, entries
69 with legends, oligomers and protein complexes. At the end we prepared a dataset consists of 363686 amide protons from 4670
70 entries. We combined the chemical shift information from BMRB and the geometric information from PDB for each amide proton
71 and its nearest aromatic ring using sequence number and residue name. For each assigned amide chemical shift, Z-score was
72 computed characterizing the deviation of the shift from its mean value from the BMRB database

$$73 \quad Z = \frac{\delta_{res} - \bar{\delta}_{res}}{\sigma_{res}} \quad (1)$$

74

75 where δ_{res} is the amide chemical shift of a given residue in ppm, $\bar{\delta}_{res}$ and σ_{res} are the mean and the standard deviation of the amide
76 proton of a given residue type, based on statistics maintained by BMRB (https://bmrb.io/ref_info/stats.php?restype=aa&set=filt).
77 For each assigned amide, the distance from the amide position to the centre of the nearest aromatic ring is computed from the
78 coordinates in the PDB mmCIF file. The distance is defined as the average of the distance from the amide proton to the centre of
79 the aromatic ring, averaged over the members of the structural ensemble present in the PDB entry. For the nearest aromatic ring,
80 we calculated an azimuth angle (Figure 1), defined as the angle between a vector normal to the aromatic ring plane and the vector
81 between the amide proton and the centre of the ring. The ring normal vector is computed by calculating the cross product of two
82 vectors on the plane of the ring (say the vector from the centre of the ring to CG and CD1). The table of assigned chemical shifts,
83 Z-scores, distances to the nearest aromatic ring and azimuth angles is provided as a comma-separated text file (CSV file) in the
84 supplementary information. The workflow used in the analysis is depicted in Figure 2.



85



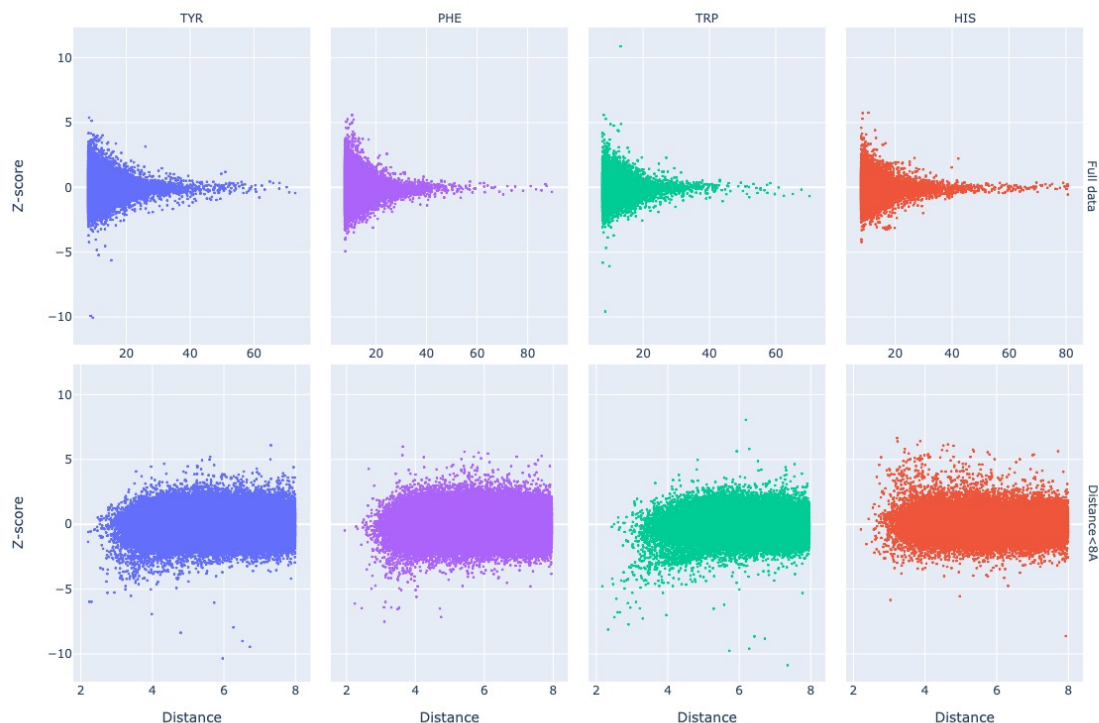
86 **Figure 2:** Manual federation of BMRB and PDB via a customized workflow.

87 Corroboration of close proximity between an amide proton and an aromatic ring observed in PDB structures is found in assigned
88 distance restraints based on nuclear Overhauser effects (NOEs) present in the BMRB entries. NMR restraint files were downloaded
89 from the PDB and parsed using PyNMRSTAR (Smelter et al., 2017) for NOE restraints between amide protons and aromatic ring
90 protons of different residues. Because many files list NOEs under ‘simple’ distance restraints, these were included. Due to
91 inconsistencies prevalent in the restraint data, several criteria were implemented to ensure some conformity in the restraints
92 included in our analysis. This and other reasons for excluding entries from the restraints analysis are described in greater detail in
93 Supplementary Table 1. Also discarded were individual distance restraints which reported only a lower distance bound or an upper
94 distance bound greater than 6Å (as this is inconsistent with the nuclear Overhauser effect) and restraints that were ambiguously
95 between more than two different residues (in order to simplify the analysis). Of the entries that remained, 2564 listed at least one
96 restraint between an amide proton and an aromatic ring proton and 863 did not.

97 3 Results and Discussion

98 3.1 Analysis of Chemical Shift Data

99 Chemical shift Z-scores as a function of distance to the nearest aromatic ring are shown in Figure 3, separated by the type of
100 aromatic sidechain. For all four aromatic residue types, there is a clear correlation between proximity to the aromatic ring and the
101 amide chemical shift variance: significant deviations from the mean, corresponding to Z-scores greater than 2, are most likely
102 when the proton is proximal to an aromatic ring, and the magnitude of the shift deviations are larger for closer proximity. The
103 bottom row in Figure 3 examines the distribution of amide chemical shifts that are closer than 8 Å in greater detail.

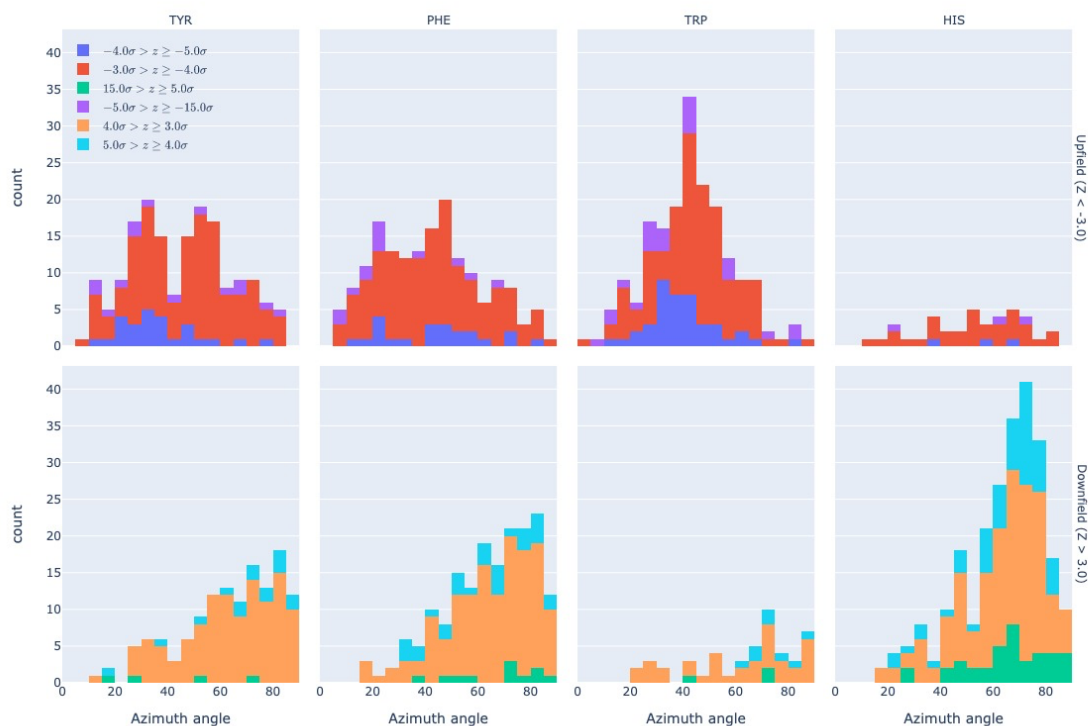




105 **Figure 3:** The distribution of amide chemical shifts as function of distance from the center of the nearest ring.

106

107 The figure illustrates differences in the pattern of chemical shift deviation for the four different types of aromatic sidechains. For
108 amide protons proximal to Phe, Tyr, or Trp sidechains, there is a noticeable preponderance of upfield shifts (negative Z-score). In
109 contrast, His amide protons exhibiting large deviations from the mean tend to be shifted downfield (positive Z-scores). The
110 difference in behavior of the outliers for the different aromatic residue types suggests the deviations are not simply the result of
111 residues buried in the protein interior. The upfield-shifted resonances for amides proximal to Phe, Tyr, and Trp are consistent with
112 hydrogen bonding between the amide and the p- π electrons. The downfield-shifted resonances for amides proximal to His
113 are consistent with hydrogen bonding to the electronegative nitrogen atoms of the His ring. In-plane downfield ring current shifts
114 are the same sign as the expected downfield shifts arising from hydrogen bonding, with a predicted amide proton ring current shift of
115 0.5 ppm for an amide nitrogen distance of 3.4 Å. This is consistent with the observation of larger magnitude Z scores for downfield-
116 shifted amide protons proximal to His.



117

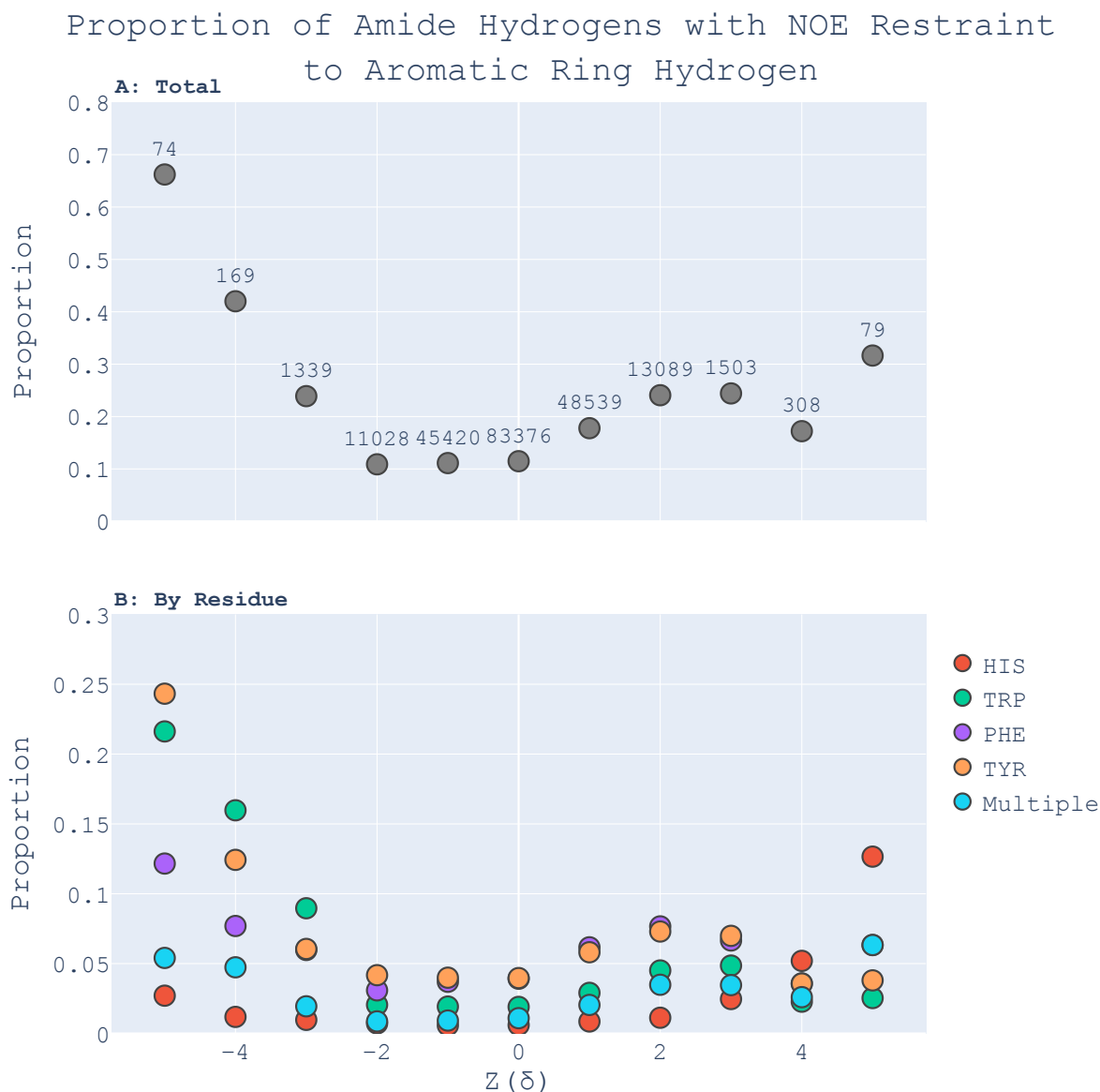
118 **Figure 4:** Distribution of azimuth angles for outlier ($>3\sigma$) amide proton shifts. Upfield shifts are shown in the top row, downfield
119 shifts in the bottom row.

120

121 Further evidence of the unusual behavior of amide protons with unusual shifts proximal to His and Trp residues is found in their
122 spatial distribution. Figure 4 shows the distribution of azimuth angle for upfield and downfield outliers that are within 8 Å of an
123 aromatic ring. (Outliers are defined here as having absolute value of the Z-score greater than 3.) Shift outliers proximal to His tend
124 to reside near the ring plane, whereas shift outliers proximal to Trp tend to reside above the ring plane. Phe and Tyr don't exhibit
125 a pronounced preponderance of outliers above or near the ring plane.



126 3.2 Analysis of Restraint Data



127

128 **Figure 5:** Proportions of amide protons with at least one NOE restraint to an aromatic ring proton (y-axis), as a function of the
129 Z-score of the amide proton (x-axis). Proportions are calculated with respect to the total number of amide hydrogens with chemical
130 shifts reported in entries with at least one amide-aromatic restraint. The numbers over each point in panel A are the total number
131 of such amides (including those lacking any NOE restraints to a nearby aromatic) with that Z-score. In panel B, the restrained
132 amide protons are further demarcated by the type of aromatic sidechain to which they are restrained.

133

134 We found 31,746 amide protons with at least one NOE restraint to a nearby aromatic ring. Figure 5A shows the proportion of
135 amide protons (from entries with usable restraint data and at least one amide-aromatic restraint) exhibiting these restraints. For



136 both upfield- and downfield-shifted amide protons, the greater the deviation from the mean the greater the likelihood that
137 corresponding NOE restraints are observed. The trend is noticeably more pronounced for the upfield-shifted amide protons, which
138 is consistent with the formation of hydrogen bonds between the amide and the p- π electrons. The downfield-shifted amides exhibit
139 a weaker correlation, which may be indicative of other dominating effects (not necessarily due to nearby aromatic rings). Figure
140 5B further demarcates the data by the type of the nearby aromatic residue. We observe that the preponderance of amide-aromatic
141 restraints in upfield-shifted amide protons for interactions with Trp and Tyr (and to a lesser extent Phe). In contrast, amide protons
142 proximal to His residues predominate strong downfield shifts ($Z \geq 4$). This stands as further evidence for hydrogen bonding from
143 the amide to the p- π electrons in Trp, Tyr, and Phe, and to the nitrogen atoms in the His ring.





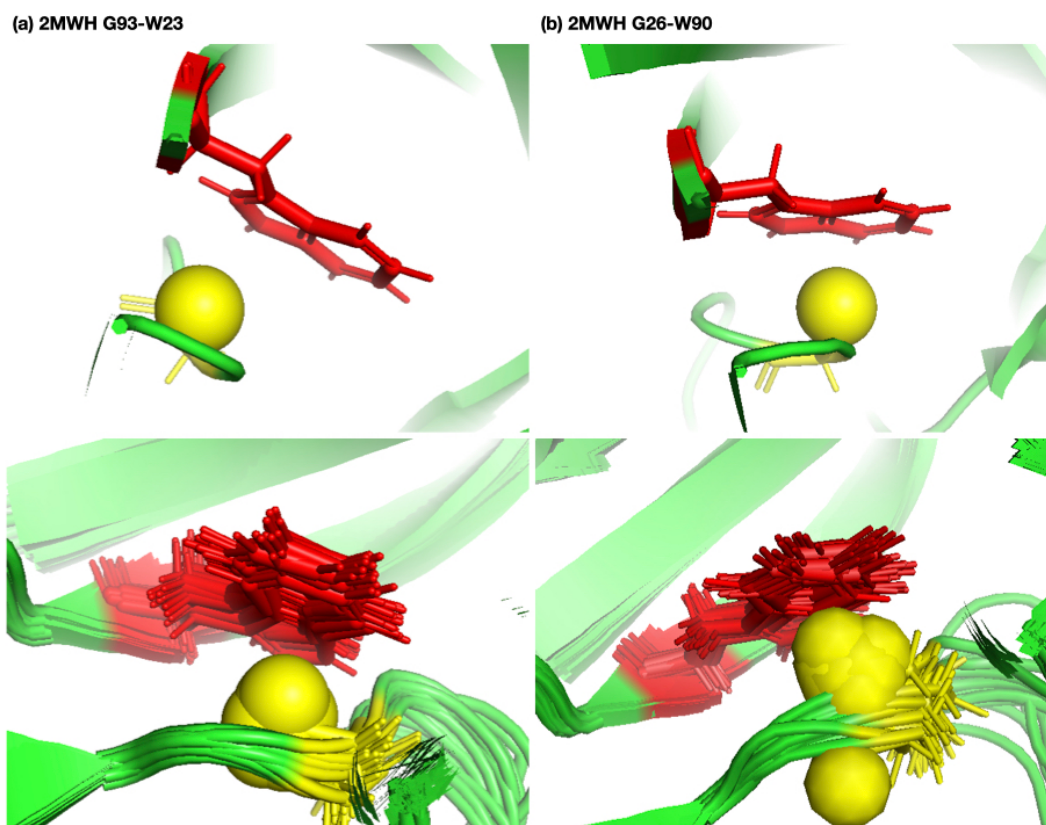
145 **Figure 6:** Shown are the number of restrained amide-aromatic pairs (that is amide protons and aromatic rings with at least one
146 defined restraint between them) for the four aromatic residue types and three Z-score classifications: upfield ($Z \leq -2$), downfield
147 ($Z \geq 2$), and normal ($-2 \leq Z \leq 2$). The colors of the bars correspond to the number of restraints between the pairs.

148

149 In Figure 6 the restrained amide-aromatic pairs are separated by the type of the aromatic residue and the number of restraints
150 between the amide proton and the aromatic ring protons. For every aromatic type, a greater proportion of the upfield-shifted pairs
151 have more than one restraint between them than the downfield-shifted pairs, which may indicate a hydrogen bond from the amide
152 to the p- π electrons. his observation is consistent with the others. Finally, the prevalence of restrained pairs with an outlier amide
153 is quite high. From the 2523 entries considered, 1166 such pairs were found, nearly one such pair in every two entries.

154 3.3 Examples

155



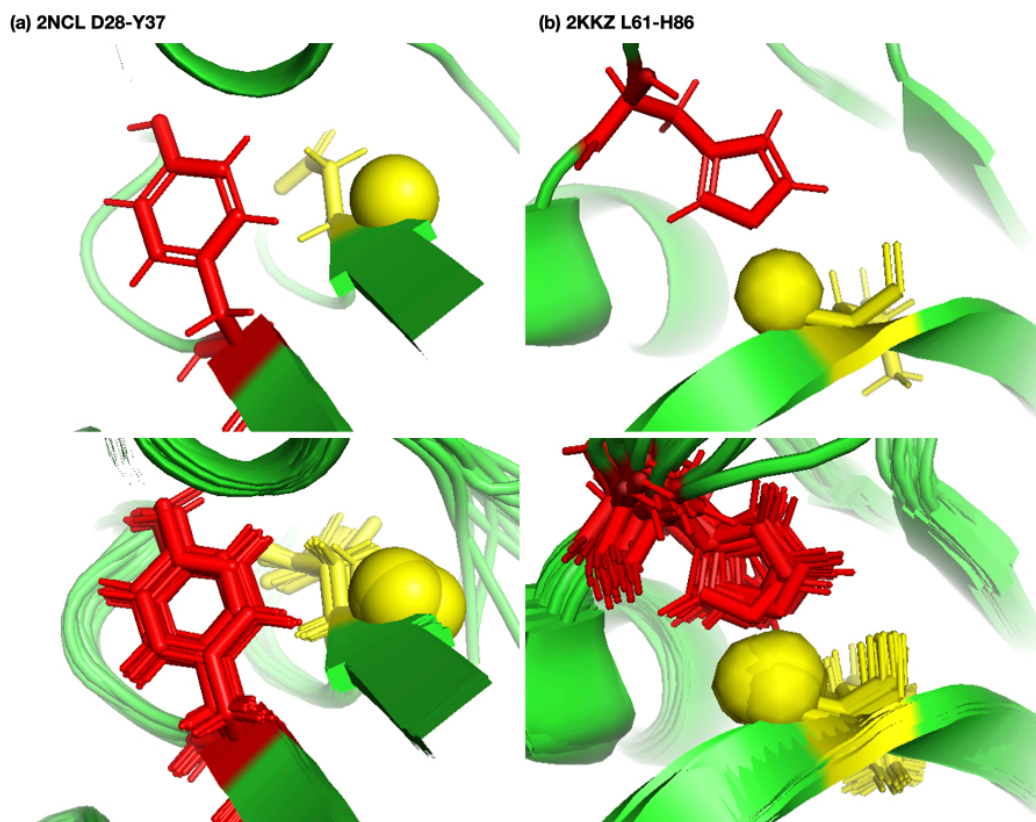
156

157 **Figure 7:** Examples of amide protons with extreme upfield shifts (a) PDB:2MWH The G93 amide proton is directly below the
158 W23 aromatic ring ($Z = -7$, $\delta_H = 2.937$ ppm), (b) PDB:2MWH The G26 amide proton is directly below the W90 aromatic ring (Z
159 $= -6.43$, $\delta_H = 3.38$ ppm). The top row shows only the first model and the bottom row shows the ensemble. The amide proton is
160 represented as a yellow sphere and the aromatic side chain is shown in red

161



162 Figure 7a & 7b shows the examples of p- π hydrogen bond in the anti-HIV lectin *Oscillatoria agardhii* agglutinin (PDB ID:2MWH)
163 in which the amide chemical shifts of G93 (z-score = -7, $\delta_H = 2.937$ ppm) and G26 (z-score = -6.43, $\delta_H = 3.38$ ppm) are upfield
164 shifted due to the interaction of W23 and W90 respectively.



165
166 **Figure 8:** Examples of amide protons with extreme downfield shifts. (a) PDB:2NCL The D28 amide proton is near the plane of
167 Y37 aromatic ring ($Z = 5.21$, $\delta_H = 11.387$ ppm), (b) PDB:2KKZ The L61 amide proton forms a hydrogen bond with the side chain
168 nitrogen of H86 ($Z = 6.66$, $\delta_H = 12.66$ ppm). The top row shows only the first model and the bottom row shows the ensemble. The
169 amide proton is represented as a yellow sphere and the aromatic side chain is shown in red.

170

171

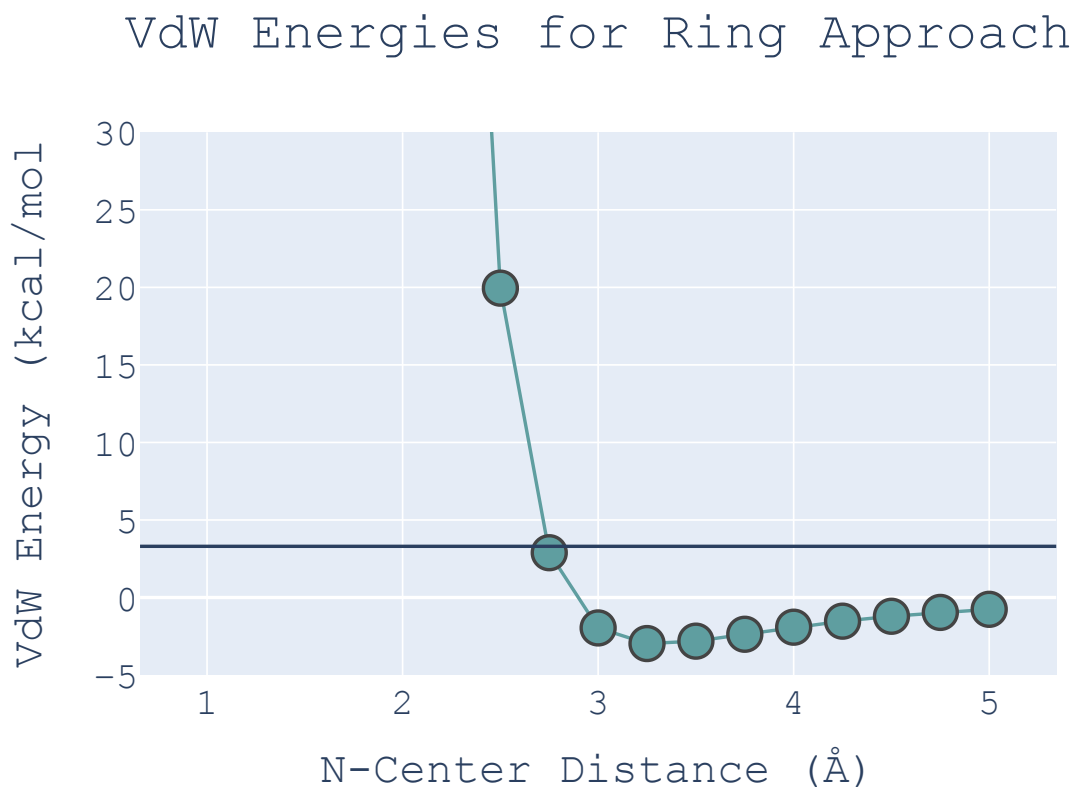
172 Figure 8a shows the amide proton of D28 is more or less on the plane of the Y37 aromatic ring in BOLA3 protein (PDB ID:2NCL)
173 resulting in the amide chemical shift of D28 (z-score = 5.21, $\delta_H = 11.387$ ppm) to shift downfield. Figure 8b shows an example of
174 possible hydrogen bond between the NE2 of H86 and the amide proton of L61 in NS1 effector domain (PDB ID:2KKZ). As a
175 result, L61 (z-score = 6.66, $\delta_H = 12.66$ ppm) amide chemical shift is strongly downfield shifted.

176 3.4 Bias, Structure, and Dynamics

177 Potential bias in the BMRB and PDB data likely undercounts the occurrence of aromatic hydrogen bonds. Absent assigned NOEs,
178 the likelihood that an NMR structure will reflect a hydrogen bond to a pi cloud of an aromatic ring is low, because the additive



179 force fields used to refine most NMR structures, such as X-PLOR/CNS, do not capture the favorable interaction energy. To explore
180 the Van der Waals interactions in an H-bonding geometry, we used MoSART(Hoch and Stern, 2003) to simulate ALA approaching
181 PHE with the amide N-H of the former exactly aligned with the ring normal of the latter. The AMBER99 force field(Wang et al.,
182 2000) was used to compute the energy.



183

184 **Figure 9:** Van der Waals interaction energies for ALA approaching PHE with its amide N-H aligned with the ring normal. On the
185 x-axis is the distance from the ALA nitrogen to the PHE ring center. VdW interaction energies for each distance were calculated
186 by subtracting the VdW energies of ALA and PHE in isolation from the energies calculated at that distance from one another. All
187 calculations were performed in MoSART using AMBER99 force fields.

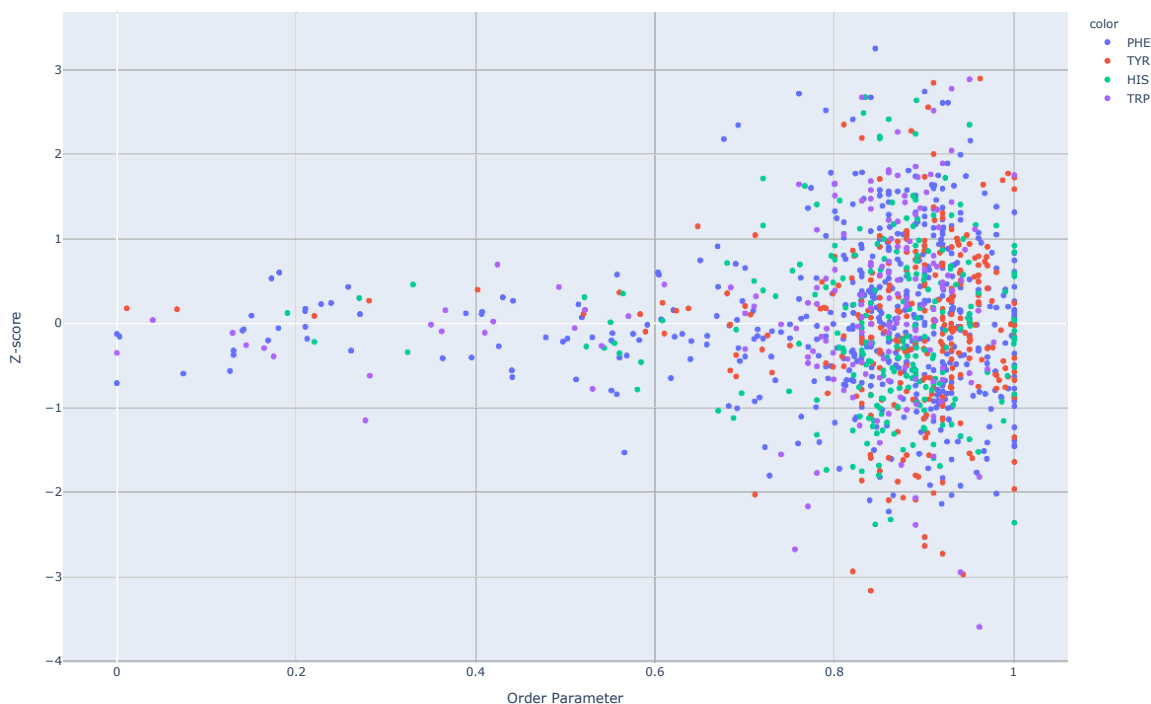
188

189 The results, shown in Figure 9, agree with those presented by Levitt and Perutz(Levitt and Perutz, 1988): there is a local minimum
190 in the van der Waals (VdW) energy with the amide nitrogen 3.3 Å from the ring center. The calculations also show that the non-
191 bonded VdW interactions do not preclude adoption of a hydrogen-bonded aromatic ring, however the well depth is so small that
192 the VdW attraction alone is likely insufficient to yield a favorable H-bond geometry without additional restraints.

193 Lack of assignments are not evidence of the absence of an NOE. Missing assignments (for example, 6280 out of 8111 outlying
194 amide proton shifts($|Z|>2$) do not have assigned NOEs to an aromatic ring) also would lead to an undercount. Possible bias in
195 BMRB notwithstanding, such as missing assignments not uniformly distributed, trends in shifts and NOE restraints for different



196 amino acid types that mirror one another provide a form of cross-validation and suggest that the shift outliers are not simply the
197 result of being buried in the protein and thus easier to assign. Bias in PDB NMR structures could reflect current practice in structure
198 refinement, which is dominated by restrained molecular mechanics simulations using empirical force fields augmented with
199 experimental restraint potentials. The forms of these restraint potentials can introduce bias (Hoch and Stern, 2005), and the additive
200 potentials that are used do not explicitly model p- π hydrogen bonds. Absent NOE or ring current restraints, NMR structures are
201 likely to under-represent aromatic hydrogen bonds.



202

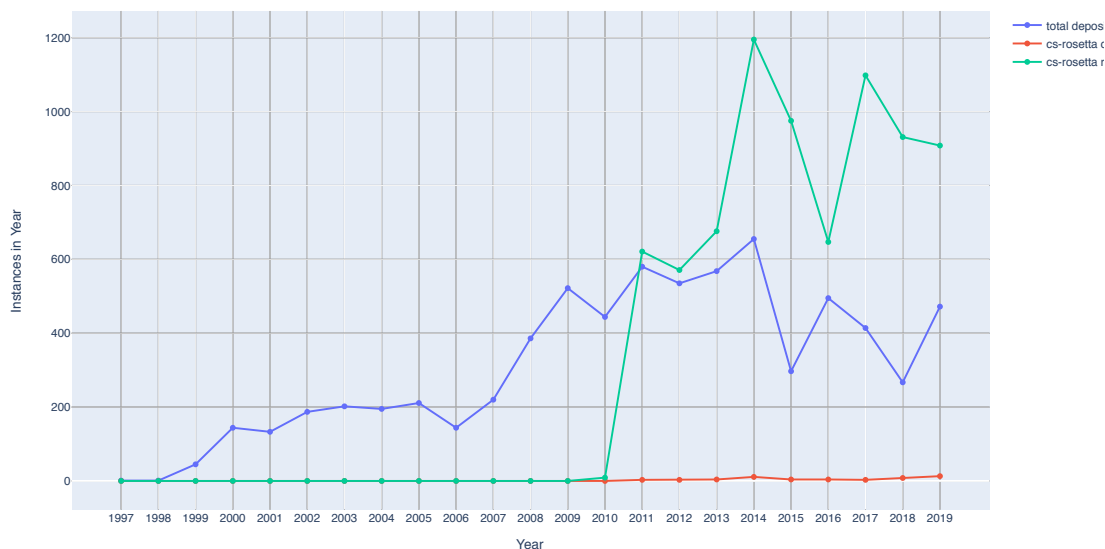
203 **Figure 10.** Correlation of Z-scores with order parameters.

204

205 In general, dynamics and disorder render chemical shifts toward their random-coil or median values (Dass et al., 2020; Nielsen
206 and Mulder, 2020). The correlation between secondary shift and order parameters is sufficiently strong that it has been used to
207 predict order parameters from chemical shifts (Figure 10). (Berjanskii and Wishart, 2005) Ring current effects in particular are
208 diminished by fluctuations about the χ_2 torsion angle. (Hoch et al., 1982) Hydrogen bonds involving aromatic rings should diminish
209 these torsional fluctuations and should find correlates in side-chain relaxation properties for aromatic residues. Solution NMR
210 structures in general tend to be more flexible than crystal structures (Fowler et al., 2020), and inclusion of hydrogen bonding
211 interactions between amide groups and aromatic rings could reduce the flexibility and potentially improve the accuracy of NMR
212 structures.



213 Although chemical shifts have been used to refine protein NMR structures (Shen et al., 2009; Berjanskii et al., 2015; Cavalli et al.,
214 2007), for the most part these approaches leverage the influence of backbone torsion angles on chemical shifts, and do not consider
215 the influence of nearby sidechains. Despite evidence that chemical shift refinement software is being used more frequently, the
216 pace of chemical shift-refined structure depositions remains low (Figure 11).

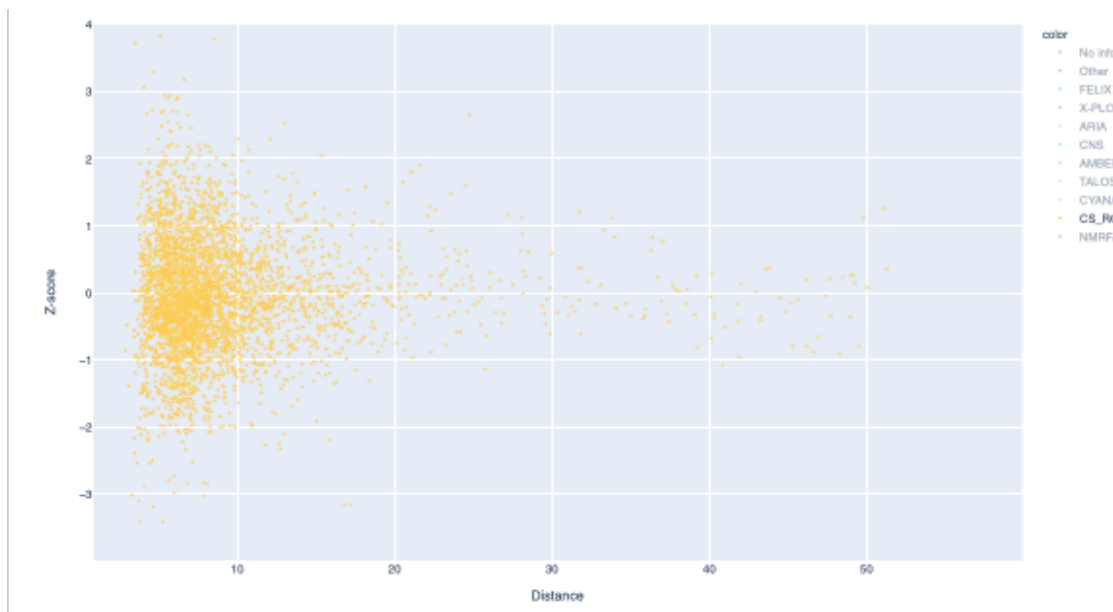


217

218 **Figure 11.** Trends in total BMRB structure depositions (blue), runs executed using the BMRB CS-Rosetta server (green), and
219 depositions citing CS-Rosetta (red).

220

221 Filtering the data plotted in Figure 3 to include only structures that reference CS-Rosetta (Figure 12) does not alter the overall
222 distributions. A challenge confronting a deeper understanding of these effects is that the available metadata in BMRB does not
223 articulate workflows, for example whether CS-Rosetta is used to generate initial trial structures or as a final refinement step), nor
224 does it indicate when ring current shift restraints were utilized.



225

226 **Figure 12.** The distribution of amide chemical shifts for depositions citing C S-Rosetta as function of distance from the center of
227 the nearest ring (compare Figure 3).

228 4 Concluding Remarks

229 Ring current shifts have a long history of providing structural insights from NMR studies of globular proteins (Perkins and Dwek,
230 1980), especially for methyl groups, whose secondary shifts tend to be dominated by ring current shifts. Early studies were largely
231 anecdotal, focusing on individual proteins or small surveys. While relatively dynamic aromatic rings (for example Tyr and Phe
232 rings that undergo ring flips on the fast exchange time scale) and disorder diminish the influence of ring current effects on secondary
233 shifts (Hoch et al., 1982), the accumulation of data in BMRB for folded proteins has provided a wealth of amide chemical shifts
234 exhibiting large secondary chemical shifts. Federation of BMRB chemical shift data with structural data from PDB confirms the
235 strong correlation between proximity to an aromatic ring and extreme secondary shifts. Markedly different secondary shift trends
236 for different aromatic residue types suggests promising avenues for improving proteins structure determination by NMR. Though
237 chemical shift refinement has been repeatedly demonstrated (Perilla et al., 2017), it has not yet been widely adopted.

238

239 The extreme outlier amide chemical shifts and corroborating NOE effects examined here provide strong evidence of the widespread
240 existence of amide-aromatic hydrogen bonds, but they are not fully conclusive. Nonetheless potential for under-representation in
241 the BMRB data exists because of incomplete assignments. Relaxation studies on ring dynamics, contrasting rings where evidence
242 suggests the presence of hydrogen bonding with rings lacking such evidence, could provide additional corroboration. Molecular
243 mechanics simulations and structure refinement using polarizable force fields could reveal additional aromatic hydrogen bonds
244 and restricted ring dynamics in folded proteins. We have initiated investigations along some of these lines.

245

246 More broadly, this preliminary investigation highlights the potential for unlocking latent knowledge hidden in BMRB, PDB, and
247 other biological databases. The challenges posed include curation and validation of the data repositories and federation of data



248 between repositories. Robust and efficient solutions to these challenges are needed in order to realize the full promise of emerging
249 methods in Machine Learning. (Hoch, 2019)

250

251 **5 Acknowledgements**

252 This work was supported by a grant from the Miriam and David Donoho Foundation, and by grants from the US National Institutes
253 of Health (R01GM109046; P41GM111135) and from the University of Connecticut Office of the Vice President for Research
254 (CARIC). We thank Milo Westler and Charles Schwieters for helpful discussions.

255



256

257

258

259 **References**

260

- 261 Armstrong, K. M., Fairman, R., and Baldwin, R. L.: The (i, i + 4) Phe-His interaction studied in an alanine-based alpha-
262 helix, *J Mol Biol*, 230, 284-291, 10.1006/jmbi.1993.1142, 1993.
- 263 Berjanskii, M., Arndt, D., Liang, Y., and Wishart, D. S.: A robust algorithm for optimizing protein structures with NMR
264 chemical shifts, *J Biomol NMR*, 63, 255-264, 10.1007/s10858-015-9982-z, 2015.
- 265 Berjanskii, M. V. and Wishart, D. S.: A simple method to predict protein flexibility using secondary chemical shifts, *J*
266 *Am Chem Soc*, 127, 14970-14971, 10.1021/ja054842f, 2005.
- 267 Bourne, P. E., Berman, H. M., McMahon, B., Watenpaugh, K. D., Westbrook, J. D., and Fitzgerald, P. M. D.: The
268 Macromolecular Crystallographic Information File (mmCIF), *Methods in Enzymology*, 277, 571-590, 1997.
- 269 Brandl, M., Weiss, M. S., Jabs, A., Sühnel, J., and Hilgenfeld, R.: C-H...pi-interactions in proteins, *J Mol Biol*, 307, 357-
270 377, 10.1006/jmbi.2000.4473, 2001.
- 271 Brinkley, R. L. and B., G. R.: Hydrogen bonding with aromatic rings., *AIChE Journal*, 47, 948-953, 2001.
- 272 Burley, S. K. and Petsko, G. A.: Amino-aromatic interactions in proteins, *FEBS Lett*, 203, 139-143, 10.1016/0014-
273 5793(86)80730-x, 1986.
- 274 Cavalli, A., Salvatella, X., Dobson, C. M., and Vendruscolo, M.: Protein structure determination from NMR chemical
275 shifts, *Proceedings of the National Academy of Sciences of the United States of America*, 104, 9615-9620,
276 10.1073/pnas.0610313104, 2007.
- 277 consortium, w.: Protein Data Bank: the single global archive for 3D macromolecular structure data, *Nucleic Acids*
278 *Res*, 47, D520-D528, 10.1093/nar/gky949, 2019.
- 279 Dass, R., Mulder, F. A. A., and Nielsen, J. T.: ODINPred: comprehensive prediction of protein order and disorder, *Sci*
280 *Rep*, 10, 14780, 10.1038/s41598-020-71716-1, 2020.
- 281 Fowler, N. J., Sljoka, A., and Williamson, M. P.: A method for validating the accuracy of NMR protein structures, *Nat*
282 *Commun*, 11, 6321, 10.1038/s41467-020-20177-1, 2020.
- 283 Haigh, C. W. and Mallion, R. B.: Ring current theories in nuclear magnetic resonance, *Progress in Nuclear Magnetic*
284 *Resonance Spectroscopy*, 13, 303-344, [https://doi.org/10.1016/0079-6565\(79\)80010-2](https://doi.org/10.1016/0079-6565(79)80010-2), 1979.
- 285 Hoch, J. C.: The Influence of Protein Structure and Dynamics on NMR Parameters, *Chemistry*, Harvard University,
286 1983.
- 287 Hoch, J. C.: If machines can learn, who needs scientists?, *J Magn Reson*, 306, 162-166, 10.1016/j.jmr.2019.07.044,
288 2019.
- 289 Hoch, J. C. and Stern, A. S.: MoSART [code], 2003.
- 290 Hoch, J. C. and Stern, A. S.: Bayesian Restraint Potentials for Consistent Inference of Biomolecular Structure from
291 NMR Data, 2005.
- 292 Hoch, J. C., Dobson, C. M., and Karplus, M.: Fluctuations and averaging of proton chemical shifts in the bovine
293 pancreatic trypsin inhibitor, *Biochemistry*, 21, 1118-1125, 1982.
- 294 Jackson, J. D.: *Classical Electrodynamics*, 3rd, Wiley1999.
- 295 Jr., C. E. J. and Bovey, F. A.: Calculation of Nuclear Magnetic Resonance Spectra of Aromatic Hydrocarbons, *The*
296 *Journal of Chemical Physics*, 29, 1012-1014, 10.1063/1.1744645, 1958.
- 297 Klemperer, W., Cronyn, M. W., Maki, A. H., and Pimentel, G. C.: Infrared studies of the association of secondary
298 amides in various solvents., *J. Amer. Chem. Soc.*, 76, 5846-5848, 1954.
- 299 Knee, J. L., Khundkar, R. L., and Zewail, A. H.: Picosecond photofragment spectroscopy. iii. vibrational
300 predissociation of van der waals' clusters., *J. Chem. Phys.*, 87, 115-127, 1987.
- 301 Levitt, M. and Perutz, M. F.: Aromatic rings act as hydrogen bond acceptors, *J Mol Biol*, 201, 751-754, 1988.
- 302 McPhail, A. T. and Sim, G. A.: Hydroxyl-benzene hydrogen bonding: an x-ray study., *Chem. Comm.*, 7, 124-126,
303 1965.



- 304 Memory, J. D.: Ring Currents in Pentacyclic Hydrocarbons, *The Journal of Chemical Physics*, 38, 1341-1343,
305 10.1063/1.1733855, 1963.
- 306 Nielsen, J. T. and Mulder, F. A. A.: Quantitative Protein Disorder Assessment Using NMR Chemical Shifts, *Methods*
307 *Mol Biol*, 2141, 303-317, 10.1007/978-1-0716-0524-0_15, 2020.
- 308 Panigrahi, S. K. and Desiraju, G. R.: Strong and weak hydrogen bonds in the protein-ligand interface, *Proteins*, 67,
309 128-141, 10.1002/prot.21253, 2007.
- 310 Perilla, J. R., Zhao, G., Lu, M., Ning, J., Hou, G., Byeon, I. L., Gronenborn, A. M., Polenova, T., and Zhang, P.: CryoEM
311 Structure Refinement by Integrating NMR Chemical Shifts with Molecular Dynamics Simulations, *J Phys Chem B*,
312 121, 3853-3863, 10.1021/acs.jpcc.6b13105, 2017.
- 313 Perkins, S. J. and Dwek, R. A.: Comparisons of ring-current shifts calculated from the crystal structure of egg white
314 lysozyme of hen with the proton nuclear magnetic resonance spectrum of lysozyme in solution, *Biochemistry*, 19,
315 245-258, 1980.
- 316 Perutz, M. F.: The role of aromatic rings as hydrogen-bond acceptors in molecular recognition., *Phil. Trans. Royal*
317 *Soc., Series A: Phys. and Eng. Sci.*, 345, 105-112, 1993.
- 318 Plevin, M. J., Bryce, D. L., and Boisbouvier, J.: Direct detection of CH/pi interactions in proteins, *Nat Chem*, 2, 466-
319 471, 10.1038/nchem.650, 2010.
- 320 Polverini, E., Rangaraj, G., Libich, D. S., Boggs, J. M., and Harauz, G.: Binding of the proline-rich segment of myelin
321 basic protein to SH3 domains: spectroscopic, microarray, and modeling studies of ligand conformation and effects
322 of posttranslational modifications, *Biochemistry*, 47, 267-282, 10.1021/bi701336n, 2008.
- 323 Shen, Y., Vernon, R., Baker, D., and Bax, A.: De novo protein structure generation from incomplete chemical shift
324 assignments, *J Biomol NMR*, 43, 63-78, 10.1007/s10858-008-9288-5, 2009.
- 325 Smelter, A., Astra, M., and Moseley, H. N.: A fast and efficient python library for interfacing with the Biological
326 Magnetic Resonance Data Bank, *BMC Bioinformatics*, 18, 175, 10.1186/s12859-017-1580-5, 2017.
- 327 Tüchsen, E. and Woodward, C.: Assignment of asparagine-44 side-chain primary amide 1H NMR resonances and the
328 peptide amide N1H resonance of glycine-37 in basic pancreatic trypsin inhibitor, *Biochemistry*, 26, 1918-1925,
329 10.1021/bi00381a020, 1987.
- 330 Ulrich, E. L., Baskaran, K., Dashti, H., Ioannidis, Y. E., Livny, M., Romero, P. R., Maziuk, D., Wedell, J. R., Yao, H.,
331 Eghbalnia, H. R., Hoch, J. C., and Markley, J. L.: NMR-STAR: comprehensive ontology for representing, archiving and
332 exchanging data from nuclear magnetic resonance spectroscopic experiments, *J Biomol NMR*, 73, 5-9,
333 10.1007/s10858-018-0220-3, 2019.
- 334 Wang, Junmei, Ciepla, Piotr, Kollman, and A., P.: How well does a restrained electrostatic potential (RESP) model
335 perform in calculating conformational energies of organic and biological molecules?, *J. Comp. Chem.*, 21, 1049-
336 1074, 2000.
- 337 Waugh, J. S. and Fessenden, R. W.: Nuclear Resonance Spectra of Hydrocarbons: The Free Electron Model, *Journal*
338 *of the American Chemical Society*, 79, 846-849, 10.1021/ja01561a017, 1957.
- 339 Weiss, M. S., Brandl, M., Sühnel, J., Pal, D., and Hilgenfeld, R.: More hydrogen bonds for the (structural) biologist,
340 *Trends Biochem Sci*, 26, 521-523, 10.1016/s0968-0004(01)01935-1, 2001.

341